

GENERALIZED MODEL OF A MAGNETORHEOLOGICAL FLUID DAMPER FOR FLUCTUATING MAGNETIC FIELDS

BOGDAN SAPIŃSKI
ADAM PIŁAT

Department of Process Control, University of Science and Technology, Cracow
email: deep@uci.agh.edu.pl; ap@ia.agh.edu.pl

The paper investigates a generalized model of a magnetorheological fluid damper (MRD). Rheological behaviour of MR fluids is described and so is the Spencer model taking into account the effects of magnetic field fluctuations in the MRD gap on the magnitude of damping force. It is demonstrated that the Spencer model does not fully emulate the real behaviour of the MRD, especially at low current levels. Some modifications of the model are suggested, whereby a nonlinear function is introduced, enveloping the family of damping force curves. The thus formulated generalized model is then verified experimentally. The model efficiency is confirmed by investigation of MRD control in a semi-active vibration isolation system for a quarter car body.

Key word: magnetorheological fluid damper, model, identification, control

1. Introduction

Magnetorheological fluid dampers (MRDs) are semi-active devices in which damping characteristics can be continuously controlled depending on the magnetic field. For this reason, MRDs are promising devices for shock and vibration isolation in spite of strongly nonlinear dynamic characteristics, which appears to be their inherent feature (Choi *et al.*, 2001). These nonlinear characteristics are mostly a result of nonlinearity introduced by the control circuit of the MRD, consisting of ferromagnetic elements and the portion of the MR fluid affected by the magnetic field excited by the current in the coil (Sapiński, 2003). Hence, processes in MR fluids and properties of the control circuit determine the dynamic behavior of MRDs.

Among different MRDs models, the only parametric model developed by Spencer (Dyke *et al.*, 1996) exhibits functional dependence of the parameters on the applied control signal and, hence, is valid when dealing with fluctuating magnetic fields. This model captures real behaviour of the MRD over a wide range of operating conditions, however it does not provide fully useful tool for control system design (Sapiński, 2002). Therefore, in order to take the full advantage of the unique features of the MRD, a dynamic model is required, which ensures good fidelity for both system evaluation and control algorithms development.

The aim of this paper is to develop such a dynamic model of the MRD that does not share shortcomings of the Spencer model, which is valid for fluctuating magnetic fields and is useful for control system design. To confirm the effectiveness of the generalized model, a linear MRD of RD-1005 series, fabricated by Lord Corporation is considered. This MRD, shown in Fig. 1, was designed to operate in the post-yield region, at low frequencies with medium or high amplitudes.

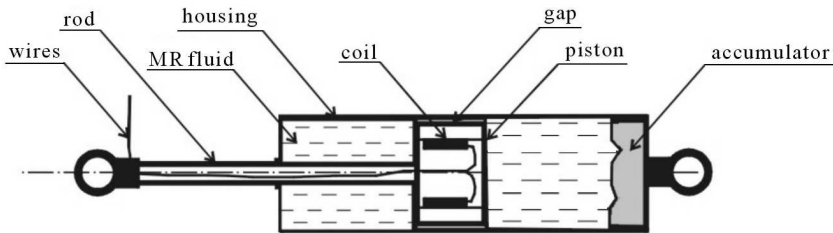


Fig. 1. Structure of RD-1005 damper

The MRD may generate any force, with the only constraint being the admissible level of the current in the coil. When no current flows through the coil, the piston motion is counteracted by the force of static friction on the piston sealing and the force due to the MR fluid flow through the gap. When the current appears in the coil, a magnetic field is generated around it. An increase in the magnetic field intensity brings about an increase in viscosity of the MR fluid present in the gap. Then the piston motion is additionally impaired by the force due to MR effect.

The MRD control uses the pulse width modulation method (PWM). It allows for shaping the control signal (i.e. current in the coil) depending on the signal frequency and PWM width. Application of PWM signals allows for the optimal selection of operating parameters of the MRD supplied from a power interface (Sapiński *et al.*, 2003).

2. Rheological behaviour of MR fluids

MR fluids are non-colloidal suspensions with micron-size, magnetically-soft iron particles dispersed in a non-magnetic fluid carrier with additives that promote homogeneity and inhibit gravitational settling. They belong to a group of non-Newtonian, rheologically stable fluids which display shear yield strength and can be controlled by a magnetic field.

The rheological properties of the MR fluid depend on the concentration of the magnetic particles, their size and shape, properties of the carrier fluid, magnetic field intensity, etc. When no separate external magnetic field exists, the particles are randomly dispersed, and the MR fluid exhibits Newtonian behaviour. In the presence of a magnetic field, the particles create chainlike structures along the field lines, which in turn create an increase of several orders of magnitude in the MR fluid viscosity. The key feature of MR fluids is the ability to reversibly change from free-flowing linear viscous liquids to semi-solid, having controllable yield strength within milliseconds, which is used in MR devices, such as dampers, clutches, brakes, etc. (Jolly *et al.*, 1999).

In terms of rheological behaviour, a MR fluid can be divided into pre- and post yield region. In the pre-yield region, the MR fluid behaves like a visco-elastic material with a complex shear modulus dependent on the magnetic field intensity H , however, in the post-yield region (Fig. 2), it exhibits properties of a visco-plastic material with the viscosity η (Bingham's model). The values of $\tau_{y,d}$ and $\tau_{y,s}$, denote the dynamic shear yield stress and the static shear yield stress which depend on H . In reality, MR fluid behaviour differs from Bingham's model, the most important difference being the non-Newtonian behaviour in the absence of a magnetic field.

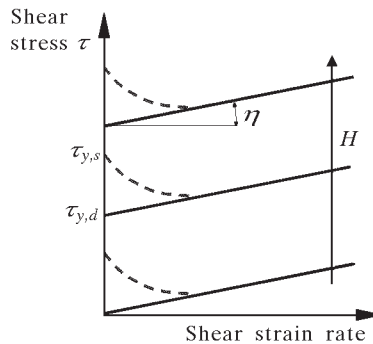


Fig. 2. MR fluid behavior in the post-yield region

3. Spencer model

The MRD model developed by Spencer captures both visco-elastic properties of the MR fluid and the appearance of a hysteresis and damping force saturation (see Fig. 3). This model is an extension of the model proposed by Bouc-Wen (Dyke *et al.*, 1996), introducing an additional dashpot c_1 and spring k_1 .

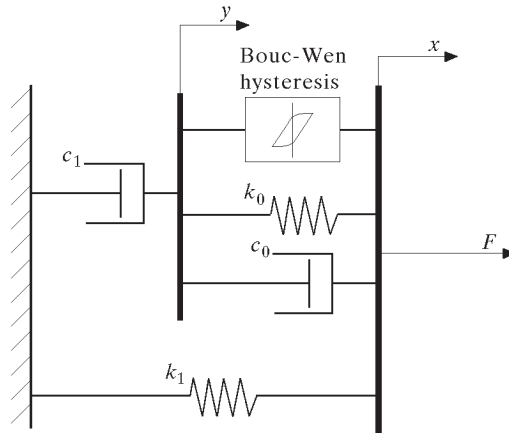


Fig. 3. Spencer model of the MRD

3.1. Governing equations

The governing equation for the Spencer model is given as

$$F = az + c_0(\dot{x} - \dot{y}) + k_0(x - y) + k_1(x - x_0) \quad (3.1)$$

It can be also written in the form

$$F = c_1\dot{y} + k_1(x - x_0) \quad (3.2)$$

The displacements z and y in equations (3.1) and (3.2) are defined by equations (3.3) and (3.4), respectively

$$\dot{z} = -\gamma|\dot{x} - \dot{y}|z|z|^{n-1} - \beta(\dot{x} - \dot{y})|z|^n + A(\dot{x} - \dot{y}) \quad (3.3)$$

$$\dot{y} = \frac{1}{c_0 + c_1}[az + c_0\dot{x} + k_0(x - y)]$$

Designations used in equations (3.1), (3.2) and (3.3) are explained below:

F	–	damping force
β, γ, A	–	parameters whose adjustment allows for shaping the linearity of the control during unloading and the smoothness of the transition from the pre-yield to post-yield area
α	–	parameter representing the stiffness for the damping force component associated with the evolution variable z
k_0	–	parameter representing the control of the stiffness of the spring at higher velocities
k_1	–	parameter representing the stiffness of the spring associated with the nominal MRD due to the accumulator
c_0	–	parameter representing viscous damping observed at higher velocities
c_1	–	parameter representing the dashpot included in the model to produce the roll off at low velocities
x_0	–	parameter representing the initial displacement of the spring with the stiffness k_0
$n = 2$	–	this value ensures satisfactory accuracy of the predicted damping force in comparison with the measured one.

The above MRD model was previously discussed and identified (Sapiński, 2002) for a given current applied, and hence the magnetic field intensity was held at a constant level. In practical applications for vibration and shock isolation, the MRD is usually employed as an actuator in the control system, and the optimal performance is expected to be achieved when the magnetic field is varied basing on the measured response of the system to which it is attached. For this reason, a dynamic model of the MRD is required, which would be capable of predicting its behaviour for fluctuating magnetic fields. To develop the model that could be useful for control system design, the functional dependence of the parameters on the applied control signal has to be determined.

In Spencer's approach, the yield stress of the MR fluid is directly dependent on the magnetic field intensity. Thus, the parameter α in equations (3.1), (3.2) and (3.3), is assumed to be a linear function of the applied control signal with a nonzero initial value at 0V (this, partly, is due to the MR fluid, which exhibits a small yield strength at the zero magnetic field for the sake of stability against gravitational settling, and partly due to the friction in the piston rod seal). Similarly, the viscous damping constants c_0 and c_1 are also assumed as linear functions of the applied control signal. Accordingly, the following functional

dependence for the parameters α , c_0 and c_1 can be written (Dyke *et al.*, 1996) as

$$\begin{aligned}\alpha &= \alpha(u) = \alpha_a + \alpha_b u & c_0 &= c_0(u) = c_{0a} + c_{0b} u \\ c_1 &= c_1(u) = c_{1a} + c_{1b} u\end{aligned}\tag{3.4}$$

where u is the control signal (voltage).

To prove the ability of the Spencer model and to reflect the MRD real behaviour for fluctuating magnetic fields, the following parameters: β , γ , A , k_0 , k_1 , x_0 , α_a , α_b , c_{0a} , c_{0b} , c_{1a} , c_{1b} have to be determined, which was done by experiments.

The following modifications to the Spencer model have been made in further considerations:

- the control signal in equations (3.4) is the current in the coil
- the damping force is given as

$$F = c_1 \dot{y} + k_1 x + F_0\tag{3.5}$$

where F_0 is the force associated with pressure in the accumulator.

3.2. Data acquisition and processing

The aim of the experiments was both to determine the influence of PWM signal parameters (frequency, PWM width factor) on the current in the coil and functional dependence of the control signal (current) on the model parameters.

The MRD experiments were conducted in an experimental setup with a computer-controlled vibration testing machine (Fig. 4).

The input-output data were acquired by using a data acquisition system which was based on a PC (Pentium III/1GHz) and multipurpose I/O board RT-DAC4 (INTECO Ltd., 2002), operating in the software environment of Windows 2000, MATLAB 6.1/Simulink and Real Time Windows Target (The Math Works Inc., 1999).

Tests were run for the mid-stroke piston position in the MRD. For the purpose of the experiments a computer program was created providing for automatic changes of the PWM signal frequency and PWM width. On the basis of registered measurement data, the relationship between the control current and signal frequency as well as PWM width was established (Fig. 5).

The model parameters: β , γ , A , k_0 , k_1 , x_0 , α_a , α_b , c_{0a} , c_{0b} , c_{1a} , c_{1b} were determined by parametric identification. For this purpose, the measured

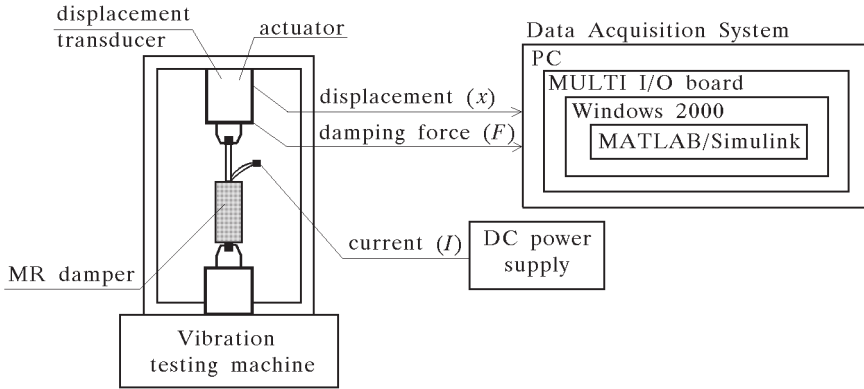


Fig. 4. Experimental setup for MRD data acquisition

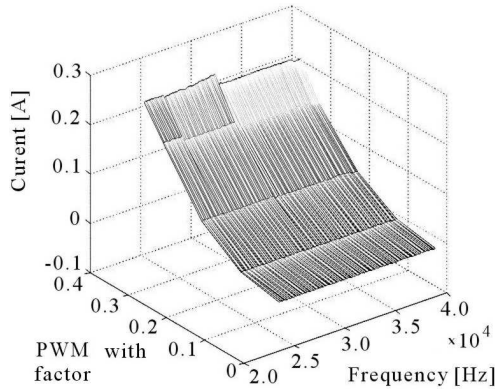


Fig. 5. Current versus PWM parameters

data of the piston displacement and current in the coil were used. Thus obtained data involved certain noise from the measured system. To minimize the optimization errors, data pre-processing was required.

The input signal, being a sine signal, can be approximated with the following function

$$g(t) = a_1 \sin(2\pi a_2 t + a_3) + a_4 \tag{3.6}$$

The approximation uses the least square method. As the ideal sine signal was considered, the piston velocity with no noise could be easily determined. The

recorded piston displacement patterns and the approximating function $g(t)$ are given in Fig. 6; the parameters of this function are

$$\begin{aligned} a_1 &= 9.9372 \cdot 10^{-3} \text{ m} & a_2 &= 0.9996 \text{ Hz} \\ a_3 &= 3.3474 \cdot 10^{-3} \text{ rad} & a_4 &= -3.3130 \cdot 10^{-5} \text{ m} \end{aligned}$$

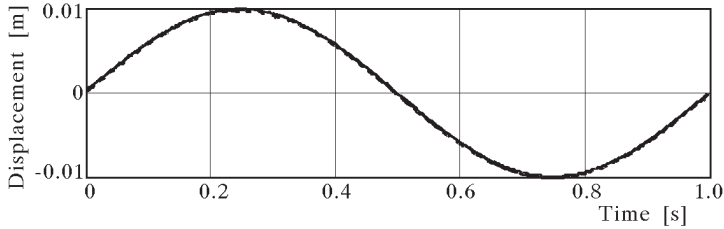


Fig. 6. Measured (---) and approximated (—) displacement signals

The input data in the optimization procedure were: level of the current, displacement approximated in accordance with formula (3.6) and velocity calculated on the basis of the approximated displacement.

3.3. Force prediction

In the first stage of the experiments the machine was programmed to generate a sinusoidal wave for six frequency levels (1.0, 2.5, 3.1, 4.1, 5.0, 6.0) Hz which corresponded to the following amplitudes $(10.0, 4.0, 3.0, 1.5, 1.2, 1.0) \cdot 10^{-3}$ m. The damping force responses (Fig. 7b) were measured for eight levels of the applied current: (0.0, 0.1, 0.2, 0.3, 0.4, 0.5, 0.6, 0.8) A (Fig. 7a).

The parametric optimization of the Spencer model was run using the nonlinear constrained optimization with the *constr* procedure available in the Optimization Toolbox of MATLAB (The Math Works Inc., 1999). The quality criterion was the integral of the squared difference between the measured and predicted force (i.e. predicted in the course of computer simulations). When the model parameters were available, the supervisory optimization algorithm started up the model simulation procedure, utilising the approximated displacement signal, (Fig. 8). The simulations yielded the damping force patterns. The error was fed back to the optimization procedure.

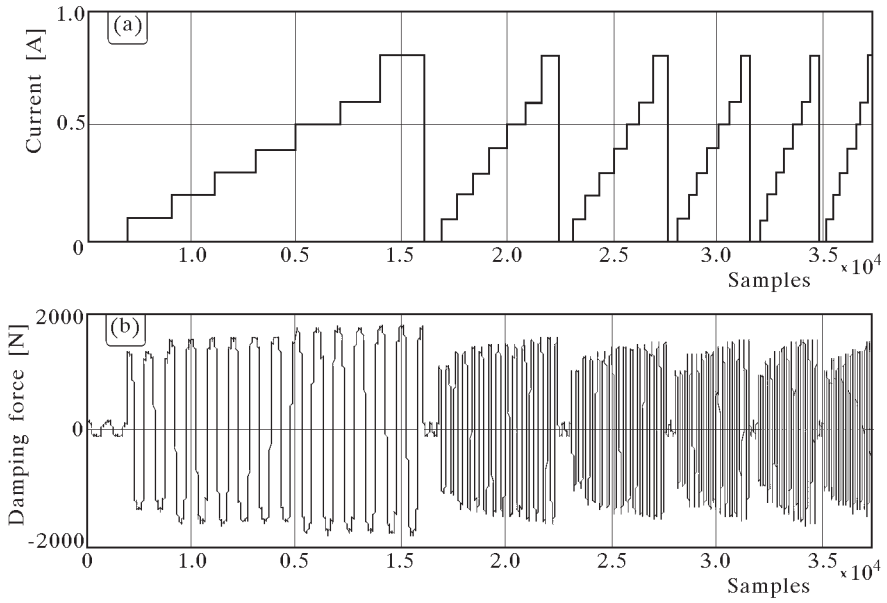


Fig. 7. Current (a) and damping force (b) for various frequencies of kinematic excitation

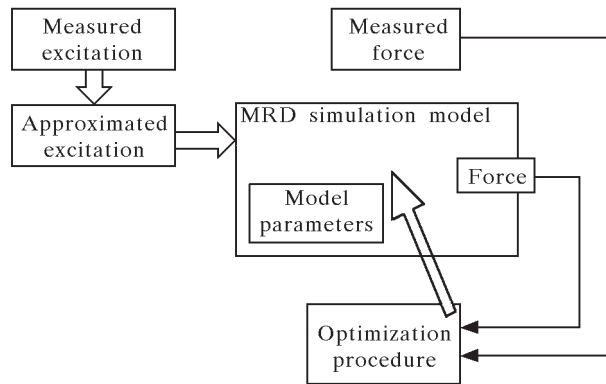


Fig. 8. Diagram of parametric optimization

The parametric optimization procedure yielded parameters of the Spencer model, summarised in Table 1.

Table 1. Parameters of the Spencer model

Parameter	Value	Parameter	Value
γ [$1/m^2$]	8130143.7364	c_{0a} [$N \cdot s/m$]	5932.5033
β [$1/m^2$]	8266348.8895	c_{0b} [$N \cdot s/(m \cdot A)$]	310.5295
A [-]	84.4652	c_{1a} [$N \cdot s/m$]	1354301.9374
k_0 [N/m]	8853.5106	c_{1b} [$N \cdot s/(m \cdot A)$]	137534.3689
k_1 [N/m]	1218.3144	F_0 [N]	260.9558
α_a [N/m]	485277.9998	$x_0 = y_0 = z_0$ [m]	0.0000
α_b [$N/(m \cdot A)$]	148549.6456		

Accordingly, computer simulations of the Spencer model were run. The results are provided in Fig. 9. Figure 9a shows the damping force patterns for the current range (0.0-0.8) A. Zoomed sections for the current 0.0 A and 0.1 A, and the kinematic excitation frequency 1 Hz and 6 Hz, are presented in Fig. 9b and Fig. 9c, respectively.

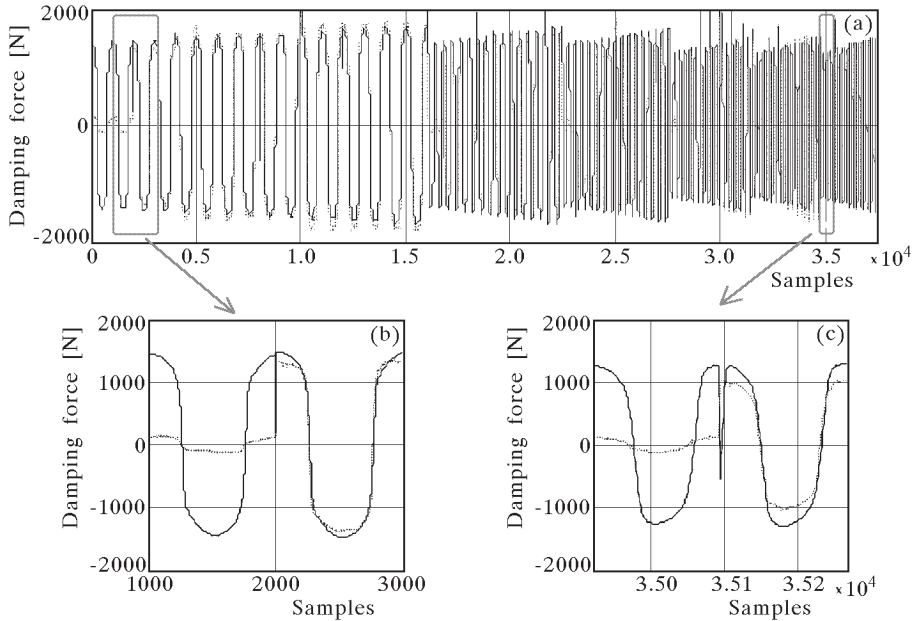


Fig. 9. Comparison of damping force patterns obtained in experiment (---) and simulation (—), in accordance with the Spencer model

The results of computer simulations reveal that the Spencer model does not emulate the real MRD behaviour throughout the tested range of control signal variations and the frequency (amplitude) of kinematic excitations, hence it proves to be inadequate for control purposes.

4. Development of a generalized model

In the light of considerations presented in Section 3, it appears that the Spencer model requires certain modifications making the model properly emulate the MRD behaviour. Major deviations of the damping force in the Spencer model occurred at zero and very small currents (0.0-0.4) A. Consistently, the measurement data were analysed again. It appeared that the envelope of the damping force patterns for small current levels was a nonlinear function (see Fig. 10). That allowed for modification of the Spencer model, given by formula (4.1). This modification led to the formulation of a generalized model which might be regarded as obligatory when dealing with fluctuating magnetic fields in the MRD gap

$$F_G = f(I)F \tag{4.1}$$

where

$$f(I) = \delta \exp(\lambda I) + 1 \tag{4.2}$$

and

- I – current in the coil
- F – damping force predicted by the Spencer model
- F_G – damping force predicted by the generalized model
- δ, λ – constant.

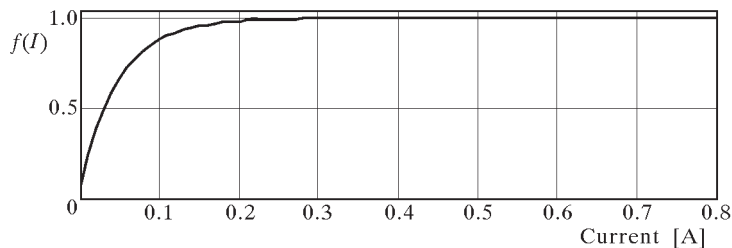


Fig. 10. Function $f(I)$

When function (4.1) is employed and the parametric optimization procedure repeated, we get the parameters of the generalized model, as provided in Table 2.

Table 2. Parameters of the Spencer model in the full operating range

Parameter	Value	Parameter	Value
γ [$1/m^2$]	8130143.7364	c_{0a} [$N \cdot s/m$]	5932.5036
β [$1/m^2$]	8266348.8895	c_{0b} [$N \cdot s/(m \cdot A)$]	310.5295
hline A [-]	84.4652	c_{1a} [$N \cdot s/m$]	1354301.9374
k_0 [N/m]	8853.5106	c_{1b} [$N \cdot s/(m \cdot A)$]	137534.3689
k_1 [N/m]	1218.3144	F_0 [N]	260.9558
α_a [N/m]	485277.9998	δ [-]	-0.9203
α_b [$N/(m \cdot A)$]	148549.6456	λ [$1/A$]	-18.3110
$x_0 = y_0 = z_0$ [m]	0.0000		

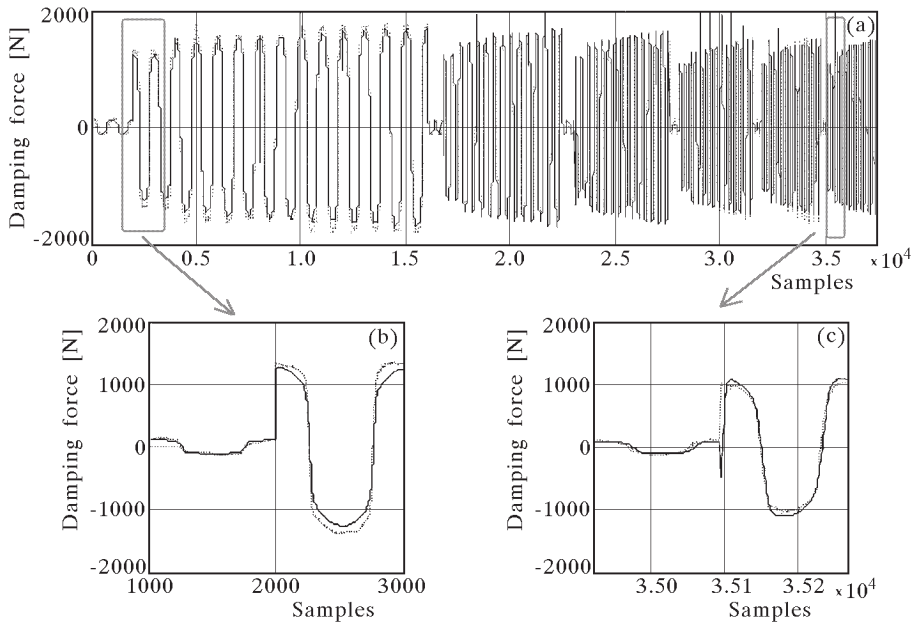


Fig. 11. Comparison of measured (- -) and predicted (—) force time patterns for the generalized model

These values were then used in computer simulations of the generalized model. The results are shown in Fig. 11. Figure 11a shows the damping force patterns for the current range (0.0-0.8) A. Zoomed sections for the current

intensity 0.0 A and 0.1 A, and the kinematic excitation frequency 1 Hz and 6 Hz are presented in Fig. 11b and Fig. 11c, respectively.

It is seen that when the linear envelope of the damping force curves is added, the Spencer model begins to correctly emulate the MRD behaviour throughout the tested range of the frequency and current levels.

The investigated damper RD-1005 is intended for truck driver seats. Together with other necessary equipment, this MRD is the key element of a vibration isolation system for the driver seat, providing adequate protection from vibrations. The results of experimental tests (Sapiński, 2003) reveal that the current level applicable to the control of the damper RD-1005 is (0.0-0.3) A. In order to formulate the dynamic MRD model, this range of the applied current was extensively tested.

For this purpose, the vibration testing machine was programmed to generate a sinusoidal wave for three frequency levels (1.0, 2.5, 5.0) Hz which corresponded to the following values of the amplitude: (10, 4, 1.2)·10⁻³ m. The responses were measured for the following levels of the applied current: (0.000-0.150) with the step 0.010 A, and (0.200-0.400) with the step 0.050 A.

The measurement results confirmed the earlier conclusions regarding the nonlinearity of the MRD damping force. It is seen in Fig. 9 that the damping force envelope is the nonlinear function given by formula (4.2). The repeated optimization procedure yielded the generalized model parameters, summarised in Table 3.

Table 3. Parameters of the generalized model in control operating range

Parameter	Value	Parameter	Value
γ [1/m ²]	8150381.3585	c_{0a} [N·s/m]	4661.23886
β [1/m ²]	8273128.2292	c_{0b} [N·s/(m·A)]	8062.2340
A [-]	168.1040	c_{1a} [N·s/m]	1461874.4425
k_0 [N/m]	8853.5105	c_{1b} [N·s/(m·A)]	183564.9655
k_1 [N/m]	1218.3144	F_0 [N]	151.8174
α_a [N/m]	418553.3227	δ [-]	-0.9436
α_b [N/(m·A)]	252504.8818	λ [1/A]	-2.0987
$x_0 = y_0 = z_0$ [m]	0.0000		

These values were then used in computer simulations of the generalized model. The results are shown in Fig. 12. Figure 12a shows the damping force patterns for the current range (0.0-0.4) A and the kinematic excitation frequency 1 Hz. Zoomed sections for the current 0.2A and 0.15A are presented in Fig. 12b and Fig. 12c.

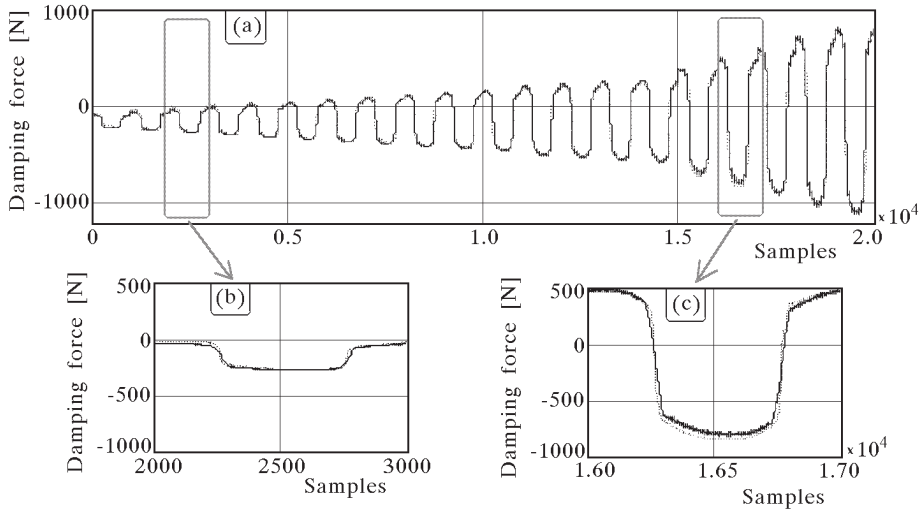


Fig. 12. Damping force obtained from experiments (---) and simulations (—) of the generalized model in the control operating range

The results confirm that the real behaviour of MRDs is fully reflected also in the range of control currents.

5. Application of the generalised model

This generalized model was then applied in simulations of a quarter-car suspension with the MRD (Sapiński *et al.*, 2003). The system performance was tested using the experimental setup shown schematically in Fig. 13.

The following values of the system parameters were assumed: wheel mass 60 kg, vehicle mass 356 kg, tire stiffness 7500 N/m, damping factor of the tire 10 Ns/m, spring stiffness 2500 N/m. As a MRD in the quarter car body the RD-1005 damper controlled by a hybrid controller was employed. The hybrid control scheme is one of the commonly used for vehicle suspensions. It allows for adjusting the damping force in the range bounded by the minimum and maximum damping. The aim of the control was to stabilize the car body position at a desired level. Mathematically, the hybrid control is a linear combination of the formulation of the skyhook and groundhook control (Ahmadian, 1999), and can be expressed as

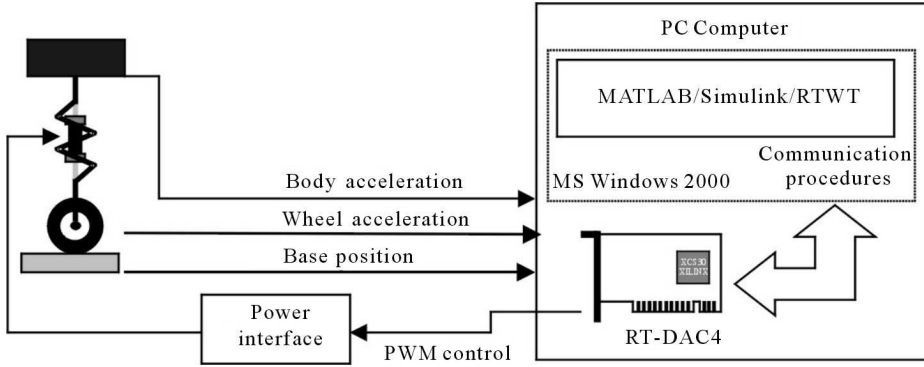


Fig. 13. Schematic diagram of the experimental setup

$$\delta_{SKY} = \begin{cases} \dot{x}_2 & \text{for } \dot{x}_2\dot{x}_0 > 0 \\ 0 & \text{for } \dot{x}_2\dot{x}_0 < 0 \end{cases}$$

$$\delta_{GND} = \begin{cases} \dot{x}_1 & \text{for } -\dot{x}_1\dot{x}_0 > 0 \\ 0 & \text{for } -\dot{x}_1\dot{x}_0 < 0 \end{cases} \tag{5.1}$$

$$v = G[\theta\delta_{SKY} + (1 - \theta)\delta_{GND}]$$

where: \dot{x}_0 – base velocity, \dot{x}_1 – wheel velocity, \dot{x}_2 – body velocity, v – control signal (PWM width factor, see Fig. 5). The variables δ_{SKY} and δ_{GND} are the skyhook and groundhook components of the damping force respectively, θ is the relative ratio between the skyhook and groundhook control, and G is a constant gain chosen experimentally such that the allowable damping force is fully utilized. If $\theta = 0$ the hybrid control reduces to the pure groundhook control, and if $\theta = 1$ the hybrid controller becomes the pure skyhook control. The constant were assumed as $\theta = 0.6$ and $G = 10$.

The input-output data were measured with a sampling frequency of 1000 Hz. The results of the measurements are shown in Fig. 14 (base excitation), Fig. 15 (car position), and Fig. 16 (control signal – PWM width factor).

The model time response was achieved for both real kinematic excitation and real control signals. The comparison of the predicted (simulation) and measured (experiment) system response indicates that the developed generalized MRD model provides sufficient accuracy in control applications.

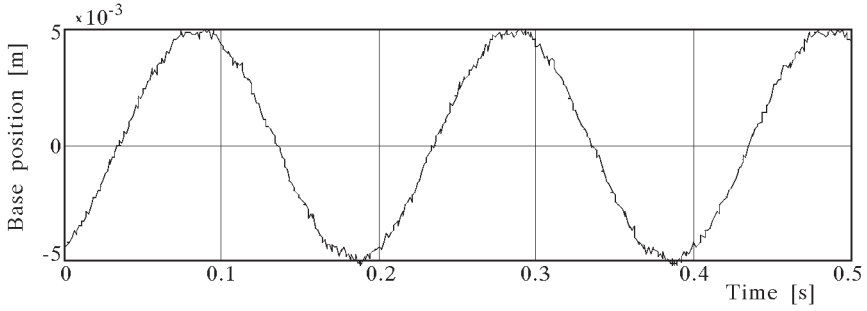


Fig. 14. Base position

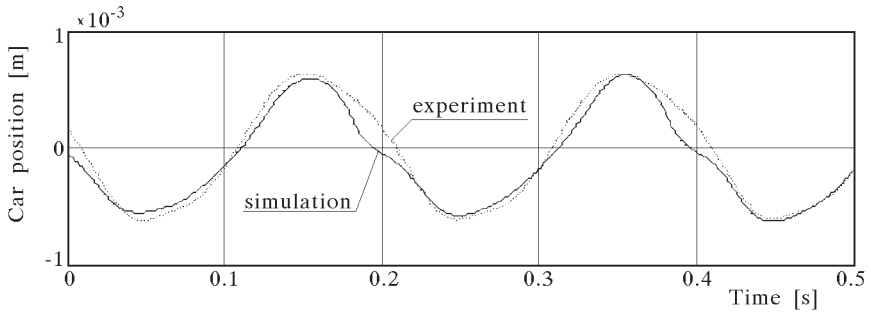


Fig. 15. Car position – generalized model

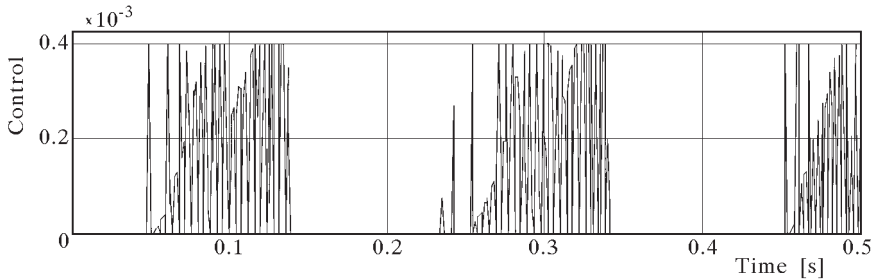


Fig. 16. Control signal – PWM width factor

6. Conclusions

The paper investigates a generalized model of the linear MRD for fluctuating magnetic fields. The model is created as a modification of the Spencer dynamic model. Although the Spencer model captures both visco-elastic pro-

properties and hysteretic behaviour of the MR fluid, it does not follow the reproduce real behaviour of the MRD with satisfactory accuracy. For this reason, it is not good enough for the development of the control algorithm.

On one hand, the shortcomings of the Spencer model were pointed out via the comparison of predicted (simulation) and measured (experiment) results. On the other, the model improvement, consisting in introducing a nonlinear function in the form of an envelope for the family curves of the damping force was presented. Such a modification of the Spencer model ensures good fidelity in portraying the actual behaviour of the MRD. For this reason, the generalized model can be successfully used in both system evaluation and control system design. The latter application was demonstrated on an example of a semi-active vibration isolation system for a quarter car body.

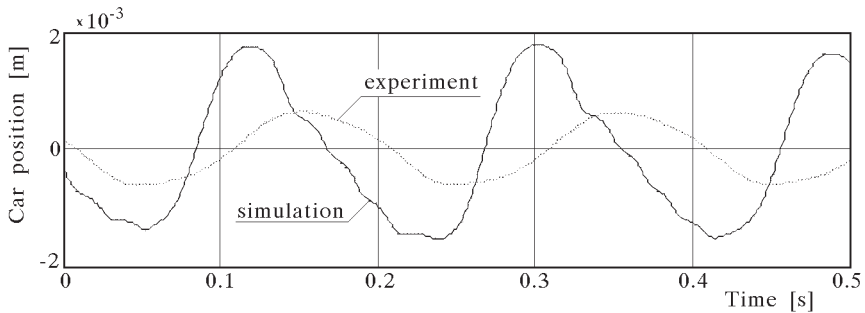


Fig. 17. Car position – Spencer model

The comparison of time responses for the closed-loop system from Fig. 15 and Fig. 17, confirms the effectiveness of the generalized model for fluctuating magnetic fields and the shortcomings of the Spencer model it used in such a case. For current levels greater than 0.4 A, the generalized model behaves like the Spencer model (see Fig. 10).

Acknowledgement

The research work has been supported by the State Committee for Scientific Research as a part of the grant No. 8T07B03520.

References

1. AHMADIAN M., 1999, On the isolation properties of semi-active dampers, *Journal of Vibration and Control*, 217-232

2. CHOI S.B., LEE S.K., PARK Y.P., 2001, A hysteresis model for the field-dependent damping force of a magnetorheological damper, *Journal of Sound and Vibration*, **245**, 375-383
3. DYKE S., SPENCER B., SAIN M., CARLSON J., 1996, Phenomenological model of a magnetorheological damper, *Journal of Engineering Mechanics*
4. JOLLY M., BENDER J.W., CARLSON J.D., 1999, Properties and applications of commercial magnetorheological fluids, *Journal of Intelligent Material Systems and Structures*, **10**, 5-13
5. SAPIŃSKI B., 2002, Parametric identification of MR linear automotive size damper, *Journal of Theoretical and Applied Mechanics*, **40**, 703-722
6. SAPIŃSKI B., 2003, Dynamic characteristics of an experimental MR fluid damper, *Engineering Transactions*, (to be published)
7. SAPIŃSKI B., PIŁAT A., ROSÓŁ M., 2003, Modelling of a quarter car semi-active suspension with MR damper, *Machine Dynamics Problems*, (to be published)
8. SAPIŃSKI B., ROSÓŁ M., 2002, Sterowniki mocy do tłumika magnetoreologicznego, *Pomiary, Automatyka, Robotyka*, **9-10**, 18-22
9. Real-Time Windows Target – User’s Guide, 1999, The Math Works Inc., Natick
10. Optimization Toolbox, 1999, The Math Works Inc., Natick
11. RT-DAC4 – User’s Guide, 2002, INTECO Ltd.

Uogólniony model tłumika magnetoreologicznego przy fluktuacjach pola magnetycznego

Streszczenie

W pracy opisano (uogólniony) model dynamiczny liniowego tłumika magnetoreologicznego uwzględniający wpływ fluktuacji pola magnetycznego w szczelinie roboczej na siłę tłumienia. Wykazano, że model ten dokładniej odzwierciedla rzeczywiste zachowanie tłumika w porównaniu z modelem sformułowanym przez Spencera. Zaproponowany model zweryfikowano eksperymentalnie. Dla potwierdzenia efektywności modelu przedstawiono przykład jego zastosowania w układzie zawieszenia pojazdu, w którym wyniki symulacji komputerowej zweryfikowano z przeprowadzonym eksperymentem.

Manuscript received April 14, 2003; accepted for print July 15, 2003